Astrocyte-Specific Deletion of Peroxisome-Proliferator Activated Receptor-γ Impairs Glucose Metabolism and Estrous Cycling in Female Mice

Marina O. Fernandez,[1,2]* Katherine Hsueh,[1]* Hyun Tae Park,[1,3] Consuelo Sauceda,[1] Vicky Hwang,[1] Deepak Kumar,[1] Sun Kim,[1] Emily Rickert,[1] Sumana Mahata,[1] and Nicholas J. G. Webster[1,4,5]

[1]Department of Medicine, School of Medicine, University of California San Diego, La Jolla, California 92093; [2]Laboratory of Neuroendocrinology, Instituto de Biología y Medicina Experimental, CONICET. Vuelta de Obligado 2490, C1428ADN, Buenos Aires, Argentina; [3]Department of Obstetrics and Gynecology, Korea University Anam Hospital, Seoul 136-705, Korea; [4]Medical Research Service, VA San Diego Healthcare System, San Diego, California 92161; and [5]Moores Cancer Center, University of California San Diego, La Jolla, California 92093

*These authors contributed equally to this study.

Mice lacking peroxisome-proliferator activated receptor-γ (PPARγ) in neurons do not become leptin resistant when placed on a high-fat diet (HFD). In male mice, this results in decreased food intake and increased energy expenditure, causing reduced body weight, but this difference in body weight is not observed in female mice. In addition, estrous cycles are disturbed and the ovaries present with hemorrhagic follicles. We observed that PPARγ was more highly expressed in astrocytes than neurons, so we created an inducible, conditional knockout of PPARγ in astrocytes (AKO). The AKO mice had impaired glucose tolerance and hepatic steatosis that did not worsen with HFD. Expression of gluconeogenic genes was elevated in the mouse livers, as was expression of several genes involved in lipogenesis, lipid transport, and storage. The AKO mice also had a reproductive phenotype with fewer estrous cycles, elevated plasma testosterone levels, reduced corpora lutea formation, and alterations in hypothalamic and ovarian gene expression. Thus, the phenotypes of the AKO mice were very different from those seen in the neuronal knockout mice, suggesting distinct roles for PPARγ in these two cell types.

Freeform/Key Words: astrocytes, fertility, glucose intolerance, obesity, PPARgamma

---

Previous studies have reported that peroxisome-proliferator activated receptor-γ (PPARγ) activation in the central nervous system (CNS) may be neuroprotective, influence energy intake and expenditure, and modulate reproductive cycles [1–6]. Consistent with these findings, PPARγ is expressed in neurons and astrocytes in key brain areas involved in cognitive function, energy homeostasis, and reproduction [7]. We previously reported that neuronal PPARγ contributes to weight gain in diet-induced obesity (DIO) and in response to rosiglitazone treatment in male mice, is essential for obesity-induced leptin resistance, and is required for the improvement of liver insulin sensitivity upon rosiglitazone treatment, suggesting effects on vagal output [4]. In female mice, we subsequently showed that neuronal

PPARγ does not alter weight gain in DIO, unlike male mice, but is still required for obesity-induced leptin resistance via the induction of *Socs3* [3]. We also showed that neuronal PPARγ is required for optimal female fertility by regulating luteinizing hormone (LH) surges and ovulation.

Although neuronal circuits regulating food intake, energy expenditure, and the hypothalamic-pituitary-gonadal axis have been the focus of intense investigation, the role of glial cells has been largely overlooked [8–10]. These cells make up 50% of the cells in the brain and comprise several important subtypes [11, 12]. Astrocytes are the most abundant glial cell in the CNS and have abundant projections resulting in a star-like morphology. They are an essential component of the blood-brain barrier, linking neurons to their blood supply, but they also support energy requirements, providing lactate and glutamine, and support neuronal function by clearing potassium and recycling neurotransmitters in synapses [13–15]. They can also become activated (astrogliosis) to form scar tissue around lesions and to clear damaged neurons. Astrocytes have an important metabolic function: 60% of glucose is converted into lactate and delivered to adjacent neurons via the monocarboxylate transporter MCT-1 [16]. Only a small proportion of brain energy (20%) comes from fatty acid oxidation, and this likely reflects lipid oxidation as an energy source for astrocytes, because the pyruvate derived from glycolysis is primarily converted to lactate for neurons, rather than entering the tricarboxylic acid cycle [16]. Recent evidence has shown that astrocytes may also play an active role in regulating peripheral metabolism [17]. Insulin signaling in astrocytes controls glucose-induced activation of POMC neurons [18], and leptin signaling in astrocytes controls feeding and obesity [19, 20]. Astrocyte inflammation is involved in promoting weight gain after a high-fat diet (HFD) feeding and loss of NF-KB signaling reduces food intake and increases energy expenditure [21, 22].

Astrocytes have also been postulated to contribute to reproductive regulation. Tanycytes, a specialized subtype of astrocyte, contact the axon termini of gonadotropin-releasing hormone (GnRH) neurons in the median eminence and modulate GnRH release [23–25]. Astrocytes can suppress postsynaptic currents in GnRH neurons [26, 27] and can produce RFRP-3, which inhibits GnRH secretion and action [28–30]. Conversely, prostaglandin E2 release from astrocytes can trigger GnRH neuron firing via EP2 receptors [31]. A functional connection is supported by physical evidence that astrocytes and GnRH neurons interact via the synaptic cell adhesion molecule 1 [32]. Given the effects of PPARγ activation in the CNS and our observation that PPARγ was expressed more highly in astrocytes than neurons, we created an inducible, conditional deletion of PPARγ in astrocytes using a GFAP-Cre-ER^T [33] mouse crossed with our PPARγ floxed mice to investigate the involvement of astrocyte PPARγ in metabolism and reproduction in female mice.

1. Materials and Methods

A. Animals

Male *Pparg*flox/flox [34, 35] mice (C57Bl/6 background) were bred with female GFAP-Cre-ER^T *(GCTF-CRE)* mice (Balb/c background; Dr. Frank Kirchhoff, Max Planck Institute, Gottingen, Germany) [33] to generate female *Pparg*flox/+:*GCTF-Cre* mice, which were then bred to *Pparg*flox/flox male mice to obtain cre+ *Pparg*flox/flox:*GCTF-Cre* mice (referred to as AKO) and *Pparg*flox/flox littermate controls (referred to as WT). The *GCTF-Cre* allele was always maintained on the female side. Mice were housed in a 12-hour light, 12-hour dark cycle at 22°C with *ad libitum* access to food and water. All experimental protocols were approved by the Institutional Animal Care and Use Committee at the University of California, San Diego, and in accordance with the Guide for the Care and Use of Laboratory Animals of the National Institutes of Health. We focused on female mice in this study to compare the effects of PPARγ loss in astrocytes with PPARγ loss in neurons that we recently reported [3].

Genotyping of the mice was performed using sequence-specific primers *Pparg-flox* and *Cre* (Supplemental Table 1). All mice used were used on the mixed C57Bl/6:Balb/c background.

Mice were fed a diet containing 400 mg of tamoxifen citrate (TAM) per kilogram, (TD.07262; Harlan Laboratories, Madison, WI) for 2 weeks starting at 11 weeks of age to induce the knockout in *Cre+* mice (termed AKO). *Cre−* mice treated with the same diet and *Cre+* mice not treated with tamoxifen were used as the control group (termed WT). Mice were then returned to a normal chow diet for another 2 weeks to allow for the metabolism and excretion of TAM before proceeding with experiments. The PPARγ knockout was confirmed by polymerase chain reaction (PCR) on genomic DNA using the primers *Pparg-recombined* (Supplemental Table 1). PCR with this primer pair gives a 230-bp product.

A-1. High-fat diet feeding and measurement of estrous cycles

Groups of AKO and WT female mice were randomly assigned to a 60% HFD to induce obesity or to a matched 10% low-fat diet (LFD; D12492 and D12450B; Research Diets, New Brunswick, NJ) for the remainder of the study. Major lipid components of the HFD are derived from lard and include 20% palmitic acid, 11% stearic acid, 34% oleic acid, and 29% linoleic acid, resulting in 32% saturated, 36% monounsaturated, and 32% polyunsaturated fat. Body weight and food intake data were recorded weekly. Female mice were evaluated for estrous cycles over 27 days by vaginal lavage starting 2 weeks after the cessation of the tamoxifen treatment or after 18 weeks on a HFD or LFD. Smears were classified as diestrus or metestrus, proestrus, and estrus on the basis of cellular morphology. A cycle was defined as a day of diestrus or metestrus followed by a day of proestrus and a day of estrus. The first 6 days of the cycling were excluded from analysis to allow the mice to acclimatize to the procedure.

B. Tissue Collection and Histology

Ovaries, brain, pituitaries, and other tissues were collected for histology and RNA extraction when the mice were killed. Paraffin-embedded sections (5 μm) were cut, dewaxed, and stained with hematoxylin and eosin. Follicle number and stage, and corpora lutea number were counted on three to five sections from ovaries from three to four mice per group and are presented as mean number per section. Follicle stages were defined as follows: Follicles were classified as primordial if they contained an oocyte surrounded by a partial or complete layer of squamous granulosa cells; as 1° if there was a single layer of cuboidal granulosa cells (GCs); as 2° if there were two or more layers of cuboidal GCs but no antrum; as early antral if there were small patches of clear space between GCs; as antral if there was a clearly defined antrum; and as atretic if there was irregular oocyte morphology. Ovarian sections examined were separated by 50 μm. Images were scanned using an Aperio ImageScope and analyzed using the Imagescope software (Leica, Buffalo Grove, IL).

C. Gene Expression

Total RNA was extracted from the tissues, using RNAbee (Tel-Test, Friendswood, TX) and RNA purification kits from Qiagen (Germantown, MD), following the manufacturers' instructions. First-strand complementary DNA was synthesized using a high-capacity complementary DNA synthesis kit (Applied Biosystems, Waltham, MA). Quantitative PCR assays were run in 20-μL triplicate reactions on an MJ Research Chromo4 instrument (Bio-Rad, Hercules, CA) or in 7-nL reactions on a BioMark HD System (Fluidigm, South San Francisco, CA). Primer sequences are listed in Supplemental Table 1. Gene expression levels were calculated after normalization to the housekeeping genes *m36B4, Gapdh*, or *RpII*, using the $2^{-\Delta\Delta Ct}$ method and expressed as relative mRNA levels compared with the control.

D. Gonadotropin Measurements

Blood (20 μL) was collected from the tail vein of female mice in EDTA-coated capillary tubes at diestrus (9:00 AM) and proestrus (6:00 PM) and plasma obtained by centrifugation. Plasma LH

and follicle-stimulating hormone (FSH) levels were measured by Luminex assay (catalog no. MPTMAG-49K; Millipore, Temecula, CA). Sensitivity of the assays was 4.9 pg/mL for LH and 24.4 pg/mL for FSH. For the GnRH and kisspeptin stimulation tests, tail-vein blood was collected before and 10 minutes (for GnRH) or 20 minutes (for kisspeptin) after intraperitoneal (IP) injection of 1 μg/kg GnRH or 30 nmol kisspeptin-10, dissolved in sterile saline solution, and gonadotropins were measured.

E. IP Glucose Tolerance and Insulin Tolerance Tests

Mice were fasted for 6 hours starting at 6:00 AM and then injected IP with glucose (1 g/kg body weight in sterile saline solution) or insulin (0.4 U/kg for normal chow and LFD, or 0.75 U/kg body weight for HFD, dissolved in sterile saline solution). Tail-vein blood glucose level was measured with a glucometer (OneTouch Ultra; Bayer Healthcare, Tarrytown, NY) at 0, 15, 30, 45, 60, 90, and 120 minutes after injection.

F. Steroid Measurements

Blood (50 μL) was drawn from the tail vein and plasma was prepared. Estrogen, progesterone, and testosterone levels were measured using a Custom Steroid Hormone Panel Kit (Meso Scale Discovery, Rockville, MD). Sensitivity of the assay was 5 pg/mL for estradiol, 70 pg/mL for progesterone, and 20 pg/mL for testosterone; the coefficients of variation were 7%, 15%, and 22%, respectively.

G. In Vivo Leptin Sensitivity Test

We measured food intake in individually housed mice injected IP with 0.5 or 1 mg/kg leptin dissolved in phosphate-buffered saline for the LFD and HFD, respectively (National Hormone and Peptide Program, Torrance, CA) at 12-hour intervals for a total of four consecutive doses. Food intake and body weight were measured throughout the 48-hour period and compared with a 48-hour period during which animals received twice daily IP injections of vehicle (phosphate-buffered saline).

H. Statistical Analysis

Data were analyzed by one- or two-way analysis of variance followed by Tukey multiple comparison posttest or Student t test, as appropriate, using Prism (GraphPad, La Jolla, CA). Normality was assessed by D'Agostino-Pearson omnibus normality test. Results were expressed as mean ± standard error and considered significant at $P < 0.05$.

2. Results

A. Detection of PPARγ in Astrocytes

Our previous immunofluorescence imaging indicated that PPARγ was expressed in neuronal and nonneuronal cells in the brain [4]. To assess relative expression, we generated primary cortical astrocyte and neuron cultures from whole brains of WT mice. PPARγ was detected in the astrocyte and the neuron cultures. The purity of the cultures was confirmed by the presence of β-3 tubulin in neuronal cultures and by the presence of glial fibrillary acidic protein (GFAP) in the astrocyte cultures. Notably, PPARγ was more robustly expressed in astrocytes than in neurons [Fig. 1(A)].

B. Deletion of PPARγ From Astrocytes

PPARγ was deleted from astrocytes by crossing *Pparg* floxed mice with mice expressing a Cre-ER^TM fusion protein under the control of the human GFAP promoter (*GCTF-CRE* mice). The
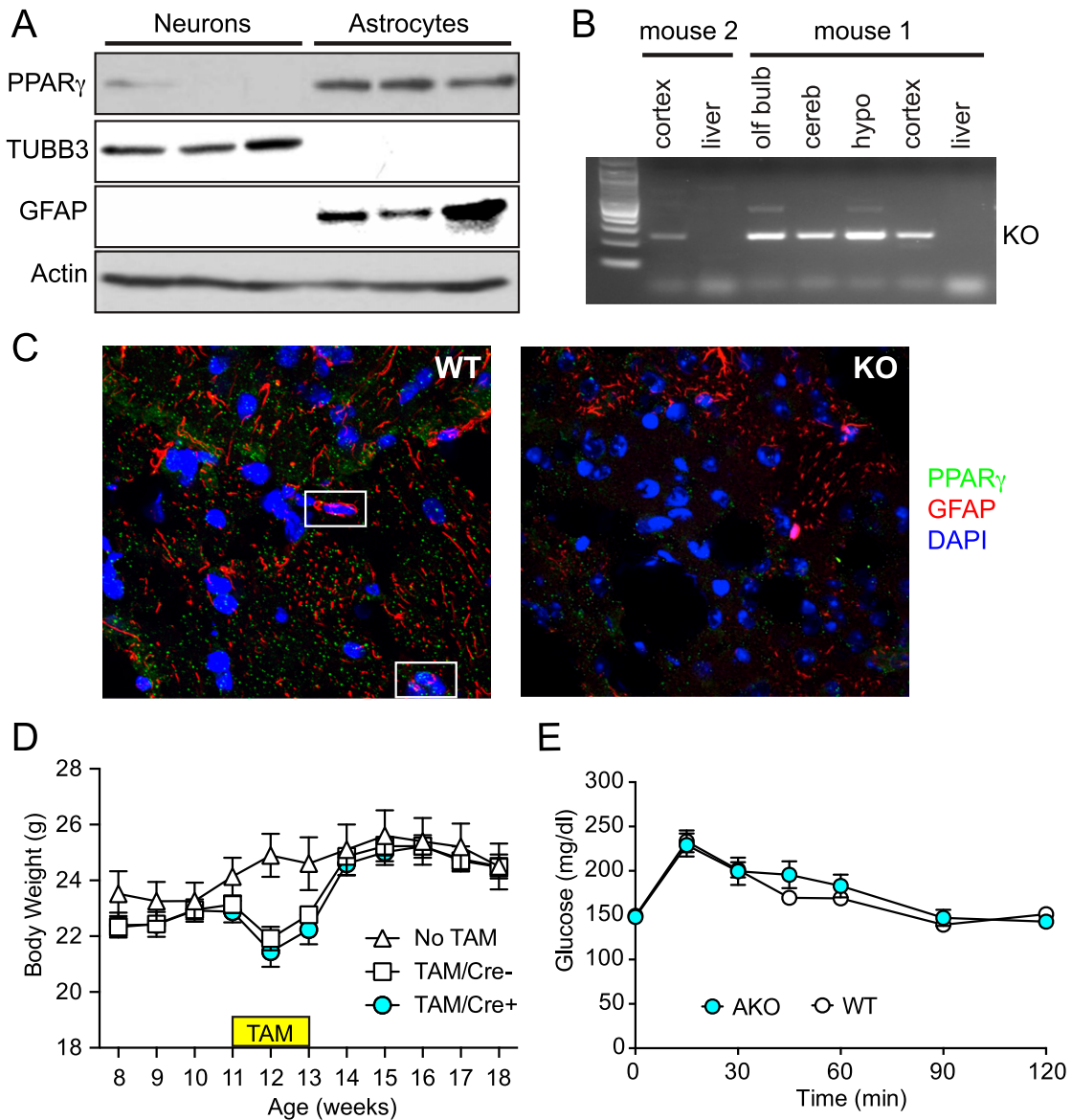
Figure 1. Inducible deletion of PPARγ in astrocytes. (A) Extracts from primary cortical neurons or astrocytes, blotted for PPARγ, the neuronal marker β-3 tubulin (TUBB3), the astrocyte marker glial fibrillary acidic protein (GFAP), or actin. (B) Recombination of *Pparg* allele in multiple brain regions but not in liver by PCR. (C) Immunofluorescent staining for PPARγ (green), GFAP (red), and DNA (blue) in sections from the nucleus accumbens of WT and AKO mice. Boxes show nuclei from GFAP-positive cells costaining for PPARγ. (D) Body weights of mice from 8 weeks to 18 weeks. Groups are *Cre*+ no TAM (white triangles; n = 8 mice), *Cre*− / TAM (white squares; n = 16 mice), and AKO knockout *Cre*+/ TAM (cyan circles; n = 24 mice). The yellow bar indicates the period of TAM treatment. Data are given as mean ± standard error of the mean. (E) Intraperitoneal glucose tolerance tests performed in female WT mice (white circles; n = 29 mice) and AKO mice (cyan circles; n = 20 mice) at 18 weeks of age. After a 6-hour fast, glucose in tail-vein blood samples was measured over 120 minutes (mean ± standard error of the mean) after a bolus of glucose (1 g/kg body weight). cereb, cerebellum; DAPI, 4′,6-diamidino-2-phenylindole; hypo, hypothalamus; KO, knockout; olf, olfactory.

fusion protein contains a mutant estrogen receptor that does not bind estrogen but binds TAM; upon addition of TAM, the Cre-ER[TM] fusion protein translocates to the nucleus to allow recombination [33]. Expression of Cre was restricted to the brain and no expression was detected in peripheral tissues (Supplemental Fig. 1A). The deleted allele was detected in the

olfactory bulb, cortex, hypothalamus, and cerebellum but not in liver, confirming the specificity of Cre expression [Fig. 1(B)]. The astrocyte knockout was confirmed by immunofluorescent staining of brain sections [Fig. 1(C)]. Punctate staining was observed for PPARγ, as previously reported [7]. PPARγ and GFAP costaining was evident in the WT mice but absent in the AKO mice. There was no evidence for recombination in the testes and ovaries (Supplemental Fig. 1A, 1B, and 1C). Body weight was monitored from 8 weeks to 18 weeks on normal chow including during the TAM treatment. The body weight of mice receiving the TAM diet decreased during the treatment but quickly recovered once the mice were returned to regular chow [Fig. 1(D)]. Glucose tolerance was tested in female mice at 18 weeks and there was no significant difference between AKO and controls receiving normal chow [Fig. 1(E)]. Nor was there a difference in insulin tolerance (Supplemental Fig. 1D). Similarly, there was no difference in glucose tolerance test (GTT) and insulin tolerance test (ITT) results for male mice (Supplemental Fig. 2A and 2B).

C. Effect of HFD-Induced Obesity on AKO Mice

Because obesity is associated with astrocyte activation, we determined whether AKO mice respond to HFD-induced obesity in the same way as WT mice. AKO and WT mice gained weight equally on the LFD or HFD [Fig. 2(A)]. Mice ate significantly more calories on the HFD in both genotypes, as would be expected, but the AKO mice fed the LFD ate less food than WT mice fed the LFD [Fig. 2(B)]. We then tested whether leptin suppression of food intake was altered. Leptin (0.5 mg/kg) suppressed food intake in WT mice fed the LFD but not in the AKO mice, because intake was already suppressed (Supplemental Fig. 2C), but a higher dose of leptin (1 mg/kg) suppressed food intake in mice fed the HFD to the same extent in both genotypes, indicating that the knockout did not alter the response to leptin. The WT mice fed the HFD were leptin resistant compared with those fed the LFD; a higher dose of leptin was required for the same decrease in food intake. The AKO mice were leptin resistant compared with WT mice when fed the LFD; interestingly, this corrected when they were fed the HFD.

GTT results after 10 weeks on diets indicated that the DIO caused glucose intolerance in WT mice, as expected. Interestingly, lean AKO mice fed the LFD were slightly glucose intolerant compared with WT mice, but obese AKO mice fed the HFD did not show any further glucose intolerance compared with lean AKO mice [Fig. 2(C)]. An intermediate effect was observed when the GTTs were performed at 4 weeks, indicating the glucose intolerance was progressive (Supplemental Fig. 3A). ITT results indicated that the AKO mice had the same initial drop in blood glucose level as WT mice fed either the LFD or HFD, but glucose values recovered faster in the AKO mice, suggesting either slight insulin resistance or faster elimination of insulin [Fig. 2(D)]. Interestingly, results of prior GTTs and ITTs of mice fed normal chow [Fig. 1(E); Supplemental Fig. 1D] showed similar trends to the LFD mice but were not significant. Histologically, the AKO mice had hepatic steatosis even when fed a LFD [Fig. 2(E)]. The average lipid droplet number was significantly higher in the WT mice fed the HFD compared with mice fed the LFD [Fig. 2(F)]. The AKO mice showed an intermediate number of lipid droplets that did not differ with diets. The lipid droplet size was larger in the WT mice fed the HFD compared with the other groups [Fig. 2(G)]; consequently, the total lipid-droplet area followed the droplet number (Supplemental Fig. 3B).

D. Altered Liver Gene Expression in AKO Mice

To assess changes in the liver, we measured gene expression by quantitative PCR in lean and obese WT and AKO female mice. Expression of genes related to gluconeogenesis (*i.e.*, *Pcx*, *G6pc*, and *Pdk4*) was increased in lean AKO mice compared with control mice and did not increase further on the HFD; only *Pck1* showed the expected HFD effect [Fig. 3(A)]. The astrocyte glutamate transporter GLT-1 (*Slc1a2*) is a known PPARγ target gene [36]; therefore, we measured expression of *Slc1a2* and the related gene *Slc1a3*. *Slc1a2* expression was decreased in AKO mice compared with that in WT mice [Fig. 3(B)], whereas there was no
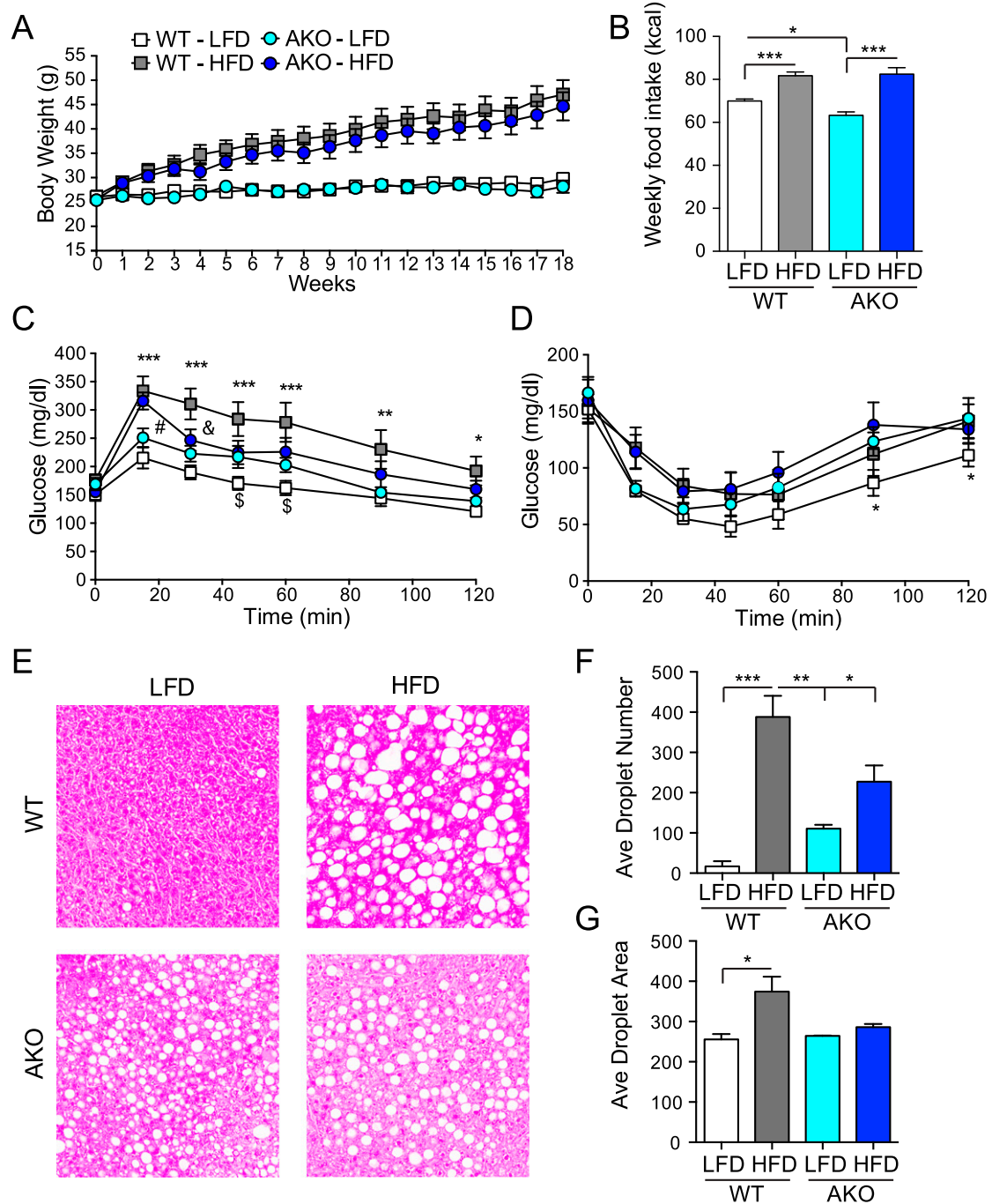
Figure 2. AKO mice were glucose intolerant but protected from the effects of the HFD. Mice were fed a 60% HFD or a matched 10% LFD for 20 weeks. (A) Body weight over time on diets [mean ± standard error of the mean (SEM)]. There were 11 WT mice in the LFD group (white bar), 13 WT mice in the HFD group (gray bar), 10 AKO mice in the LFD group (cyan bar), and 15 AKO mice in the HFD group (blue bar). Squares, WT mice; circles, AKO mice. Body weights of mice fed the HFD showed a time effect ($P < 0.0001$) but no genotype effect or interaction by repeated measures two-way analysis of variance (ANOVA). (B) Mean weekly caloric intake over 18 weeks on diets. There was a significant diet effect ($P < 0.0001$) by two-way ANOVA. *$P < 0.05$; ***$P < 0.001$. (C) IP GTTs performed in WT mice (n = 9 in the LFD group; n = 13 in the HFD group) and AKO mice (n = 9 in the LFD group; n = 15 in the HFD group) after 10 weeks on diets. After a 6-hour fast, glucose levels from tail-vein blood samples were measured over 120 minutes (mean ± SEM) after a bolus of glucose (1 g/kg body weight). WT mice showed a significant diet and time effect ($P < 0.01$ and < 0.0001, respectively) and

diet-time interaction ($P < 0.01$) by two-way ANOVA; however, AKO mice only showed a significant time effect ($P < 0.0001$) and diet-time interaction ($P < 0.05$). *$P < 0.05$; **$P < 0.05$; ***$P < 0.001$ for WT mice fed the HFD vs WT mice fed the LFD; #$P < 0.05$ for AKO mice fed the HFD vs AKO mice fed the LFD; &$P < 0.05$ for AKO mice fed the HFD vs WT mice fed the HFD. (D) ITTs performed in WT and AKO mice after 11 weeks on diets. Mice fed the LFD received 0.4 IU/kg insulin and mice fed the HFD received 0.75 IU/kg insulin after a 6-hour fast. Glucose levels in tail-vein blood samples were measured over 120 minutes (mean ± SEM). Two-way ANOVA of LFD data showed a time effect ($P < 0.0001$) and significant differences between genotypes at 90 and 120 minutes. *$P < 0.05$. HFD data also showed a time effect but no significant differences between genotypes. (E) Hematoxylin- and eosin-stained sections of livers from mice killed after 18 weeks on diets. (F) Quantification of lipid droplet number from multiple sections of livers. Data are given as mean ± SEM. Two-way ANOVA indicates a significant diet effect ($P < 0.001$) and a diet-genotype interaction ($P < 0.05$). *$P < 0.05$; **$P < 0.05$; ***$P < 0.001$ for indicated comparisons. (G) Quantification of mean lipid-droplet area from multiple sections of livers. Data are mean ± SEM; n = 3 per group. Two-way ANOVA indicates a significant diet effect ($P < 0.05$). *$P < 0.05$ for the indicated comparison. Ave, average.

difference in *Slc1a3* expression compared with that in WT mice (Supplemental Fig. 3C). Expression of the cytosolic acetyl-CoA carboxylase 1 gene (*Acaca*) that controls malonyl-CoA production for lipid synthesis was increased in the AKO mice fed the LFD and decreased in the AKO mice fed the HFD, whereas the mitochondrial acetyl-CoA carboxylase 2 gene (*Acacb*), which generates malonyl-CoA to block CPT1, showed an HFD-dependent decrease in both genotypes [Fig. 3(C)]. Other lipid biosynthetic genes did not show a genotype effect, although some showed diet effects (Supplemental Fig. 3D). These results suggested increased lipid synthesis in the AKO mice fed the LFD and increased lipid uptake/oxidation in mitochondria in the obese mice irrespective of genotype. The liver expresses high levels of the lipid transfer genes cell-death inducing DFFA-like effectors *Cideb* and *Cidec*, and the perilipin *Plin2,* with lower levels of *Cidea* and *Plin1* (Supplemental Fig. 3E). Expression of *Cidec* was increased by HFD in the WT mice but basal *Cidec* expression was elevated in the AKO mice and did not increase significantly with the HFD [Fig. 3(D)]. *Cideb* was expressed less in the AKO mice in the LFD and HFD groups and *Plin2* expression was increased with the HFD and decreased in the AKO mice [Fig. 3(D)]. *Plin1* expression showed a HFD-dependent increase in both genotypes and *Cidea* expression was elevated by HFD selectively in the WT mice (Supplemental Fig. 3F).

The changes in these genes indicated altered lipid storage in the AKO mice. Furthermore, hormone-sensitive lipase gene (*Lipe*) expression showed a similar pattern to *Cidec* expression, being increased by HFD in WT mice but basally elevated in AKO mice [Fig. 3(E)], consistent with increased hepatic lipid metabolism and storage. Expression of the low-density lipo-protein receptor gene (*Ldlr*) was increased by the HFD, consistent with increased hepatic lipid uptake via low-density lipoprotein clearance [Fig. 3(E)]; however, again, *Ldlr* expression was higher in the AKO mice and did not respond to the HFD. In contrast, the lipid transporter *Abcd2*, involved in fatty acid transport into peroxisomes, was reduced by the HFD and AKO, whereas the transporters *Crot* and *Cpt2a*, which mediate transport out of peroxisomes and into mitochondria, were increased by the HFD in both genotypes, although the response in the AKO mice was lower [Fig. 3(E)]. Last, genes related to lipid oxidation in peroxisomes (*i.e.*, *Acox1, Ehhadh*, and *Acaa1a*) or in mitochondria (*i.e.*, *Acadvl* and *Acadl*) had decreased expression in AKO mice irrespective of diet [Fig. 3(F)], as did the *Slc24a4* and *Slc24a5* mitochondrial nucleotide transport genes (Supplemental Fig. 3G).

E. AKO Mice had Altered Estrous Cycles; HFD Reversed This effect

We have reported that loss of PPARγ in neurons disrupts estrous cycles [3]. Therefore, we assessed estrous cycles in the AKO mice and WT animals fed normal chow. AKOs had significantly fewer days in proestrus and significantly fewer cycles over 3 weeks of cycling [Fig. 4(A) and 4(B)]. Example cyclegrams are shown in Supplemental Fig. 4. There were no
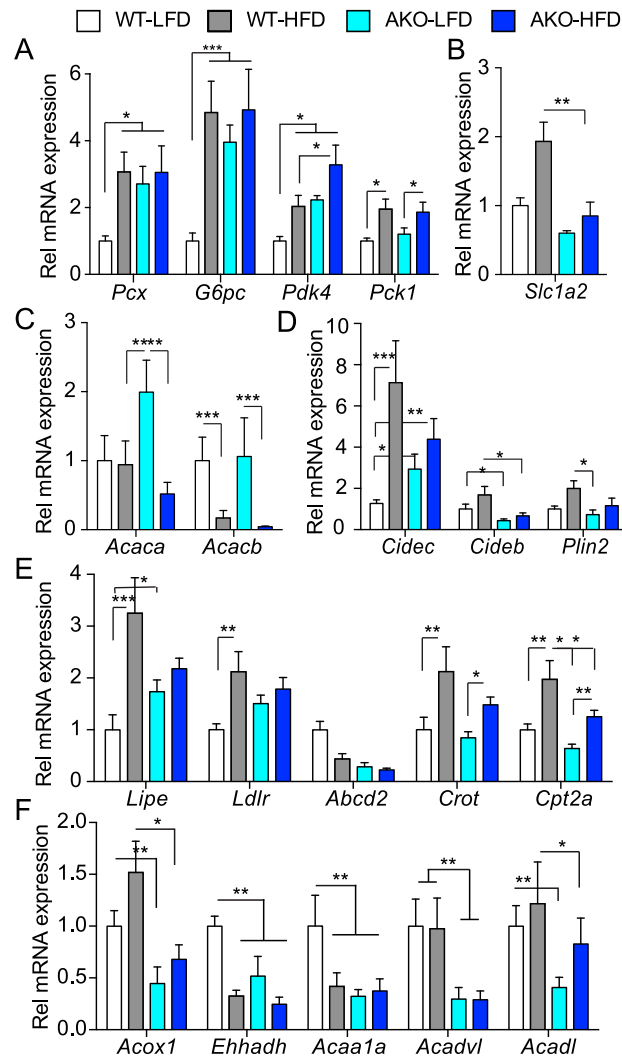
Figure 3. Alterations in liver gene expression after loss of PPARγ in astrocytes. Gene expression was measured on RNA extracted from livers by quantitative PCR when mice were killed. Data are presented as mean ± standard error of the mean; n = 6 mice per group. (A) Expression of the gluconeogenic genes pyruvate carboxylase (*Pcx*), glucose-6-phospatase (*G6pc*), pyruvate dehydrogenase 4 (*Pdk4*), and phosphoenolpyruvate carboxykinase (*Pck1*). (B) Expression of *Slc1a2*. (C) Expression of *Acaca* and *Acacb*. (D) Expression of *Cideb*, *Cidec*, and *Plin2*. (E) Expression of *Lipe*, *Ldlr*, the peroxisome fatty acid transporters *Abcd2* and *Crot*, and the mitochondrial fatty acyl-CoA transporter *Cpt2a*. (F) Expression of the peroxisomal fatty acid oxidation genes acyl-CoA oxidase 1 (*Acox1*), enoyl-CoA hydratase and 3-hydroxyacyl-CoA dehydrogenase (*Ehhadh*), and acetyl-CoA acyltransferase 1a (*Acaa1a*); and the mitochondrial genes acyl-CoA dehydrogenase very long chain (*Acadvl*) and acyl-CoA dehydrogenase long chain (*Acadl*). All gene expression was significantly different by two-way analysis of variance. *$P < 0.05$; **$P < 0.01$; ***$P < 0.001$ for the indicated *post hoc* comparisons. Rel, relative.

significant differences in diestrus LH or FSH levels in AKO mice [Fig. 4(C)]. A GnRH-stimulation test indicated that the pituitary gonadotropin response to GnRH was not different between AKO and control mice [Fig. 4(D)], with the expected increase in LH levels after GnRH stimulation in both groups.

To evaluate the effects of DIO on estrous cycles and ovarian histology, estrous cycles were monitored over 21 days in AKO and control mice that had been fed a 60% HFD or 10% LFD over 18 weeks. WT mice fed the HFD had fewer cycles over 21 days and fewer days in proestrus when compared with lean controls [Fig. 5(A) and 5(B)], consistent with our previously
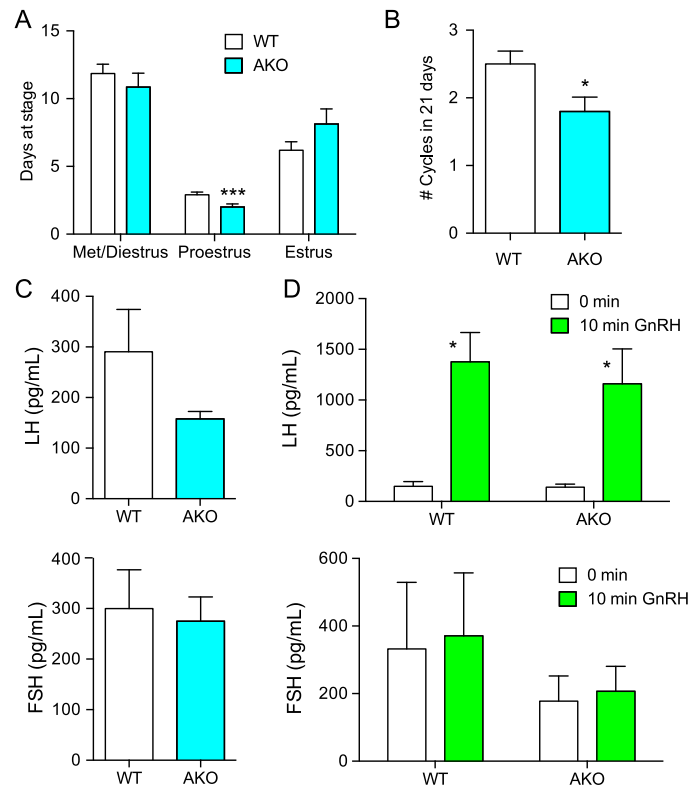
Figure 4. Alterations in estrous cycles after loss of PPARγ in astrocytes. (A) Estrous cycles of mice were staged by vaginal cytology for 21 days. WT mice, n = 22 (white); AKO, n = 22 (cyan). (B) Quantification of the number of cycles during the 21 days. (C) Plasma LH and FSH levels during the morning of diestrus (n = 10/group). (D) GnRH pituitary stimulation test. Mice received GnRH (1 μg/kg) in the morning (n = 4/group). Tail-vein blood samples were collected before (white bars) and 10 minutes after (green bars) GnRH injection. Data are shown as mean ± standard error of the mean. LH values showed a significant GnRH effect ($P < 0.05$) but no genotype effect by two-way analysis of variance. FSH values did not change significantly. Flox, floxed mice; Met/di, metestrus/diestrus.

published data [37]. AKO mice fed the LFD had the same decrease in cycle number as the WT mice fed the HFD, consistent with our initial cycling in mice fed normal chow. Surprisingly, HFD feeding normalized the reduced number of cycles and number of days in proestrus in the AKO mice [Fig. 5(A) and 5(B)].

When ovarian histology was analyzed [Fig. 5(C)], we observed that although the number of primordial follicles was reduced in control mice fed HFD, this effect was lost in AKO mice. Interestingly, lean AKO mice had more primary follicles, and the HFD reduced the numbers to those of control mice. The HFD reduced the number of corpora lutea in WT mice, as we have shown previously [37]. The lean AKO mice had significantly fewer corpora lutea than lean control mice, but obesity increased the number of corpora lutea, consistent with the cycling results [Fig. 5(D)]. These results show that a PPARγ deletion in astrocytes impairs estrous cycles similar to the HFD in WT mice, and that functional PPARγ in astrocytes is necessary for the detrimental effects of HFD.

F. AKO Mice Had Lower Diestrus LH and Higher Testosterone Levels

Gonadotropin levels were analyzed in lean and obese animals in diestrus and in proestrus. The diestrus LH level was significantly lower in both lean and obese AKO [Fig. 6(A)], but the diestrus FSH level was not significantly different [Fig. 6(B)]. LH levels in WT mice at proestrus had basal and surge values indicating that 50% of the mice (three of the six) had the proestrus surge [Fig. 6(C)]. Obesity reduced the number of surges in WT mice to 20% (one of
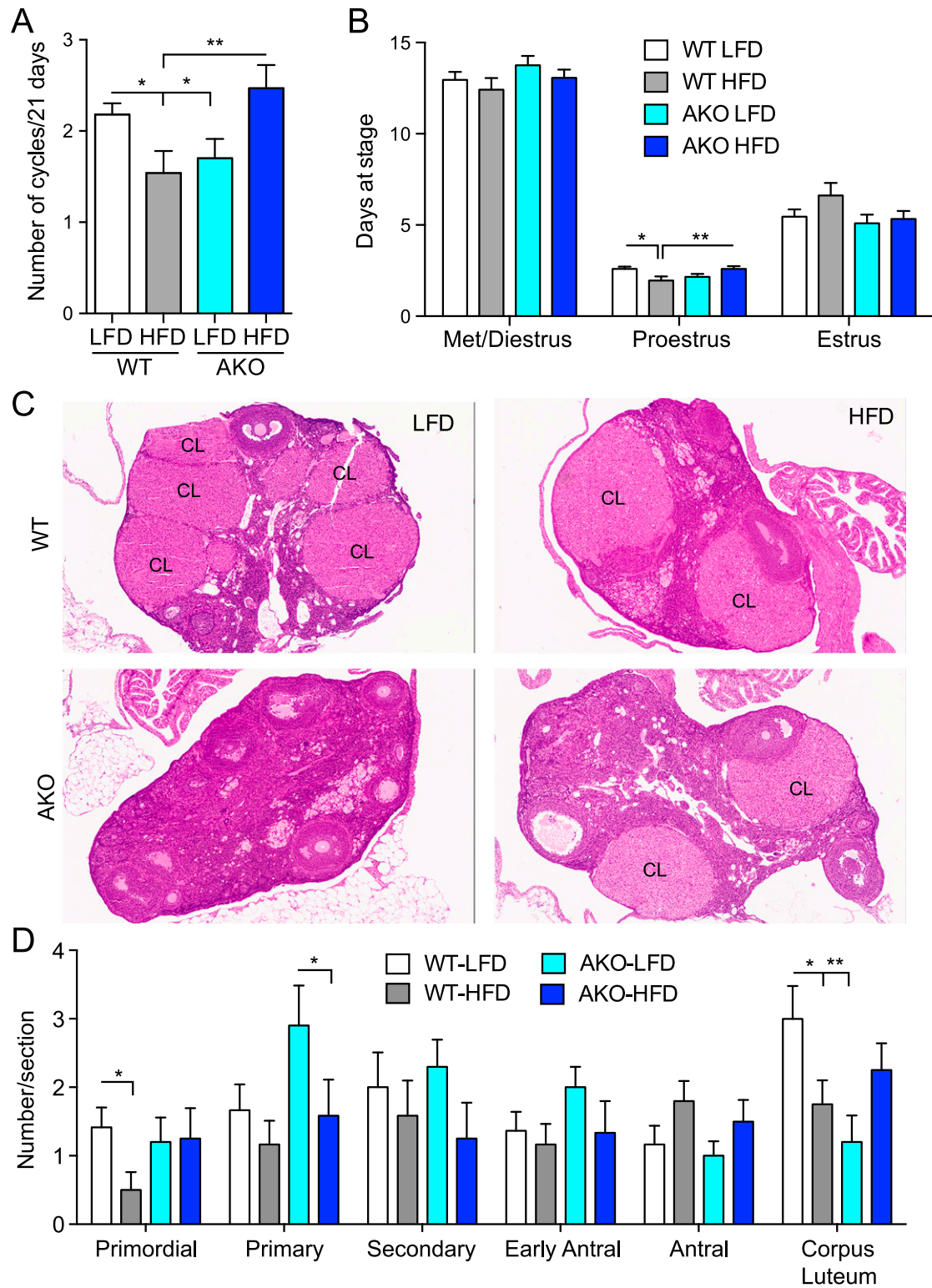
Figure 5. DIO impaired estrous cycles in WT but not AKO mice. (A) Number of cycles over time on diets for WT mice (n = 11, LFD group; n = 13, HFD group) and AKO mice (n = 10 in LFD group; n = 15 in HFD group) mice. Estrous cycles were monitored by vaginal cytology for 21 days after 15 weeks on diets. (B) Days at metestrus/diestrus, proestrus, or estrus over 21 days of cycling. (C) Ovarian morphology. Representative hematoxylin- and eosin-stained sections of ovaries (D) Quantification of follicle stage and corpora lutea. Number of follicles per three to five sections spaced by 50 μm (mean ± standard error of the mean) for WT mice

(n = 12, LFD group; n = 12, HFD group) and AKO mice (n = 10, LFD group; n = 12, HFD group) mice. Primary and antral follicles showed a diet effect ($P < 0.05$) and there was a significant diet-genotype effect for corpora lutea ($P < 0.01$) by two-way analysis of variance. Data are shown as mean $\pm$ standard error of the mean. *$P < 0.05$; **$P < 0.01$ for indicated *post hoc* comparisons. CL, corpus lutea; Flox, floxed mice.

five), as we have previously reported [37]. LH values in the lean AKO mice showed that 33% of mice (three of nine) had ovulated, and 33% (two of six) of the obese AKO mice had ovulated. Therefore, AKO mice had fewer LH surges and the occurrence of surges was not altered by obesity. In contrast, proestrus FSH levels did not vary with diet or genotype [Fig. 6(D)]. Plasma estradiol and progesterone levels at diestrus did not change with genotype or diet, but testosterone was increased in obese control mice and AKO mice compared with their lean counterparts, whereas lean AKO mice also had higher testosterone levels when compared with lean controls [Fig. 6(E)].
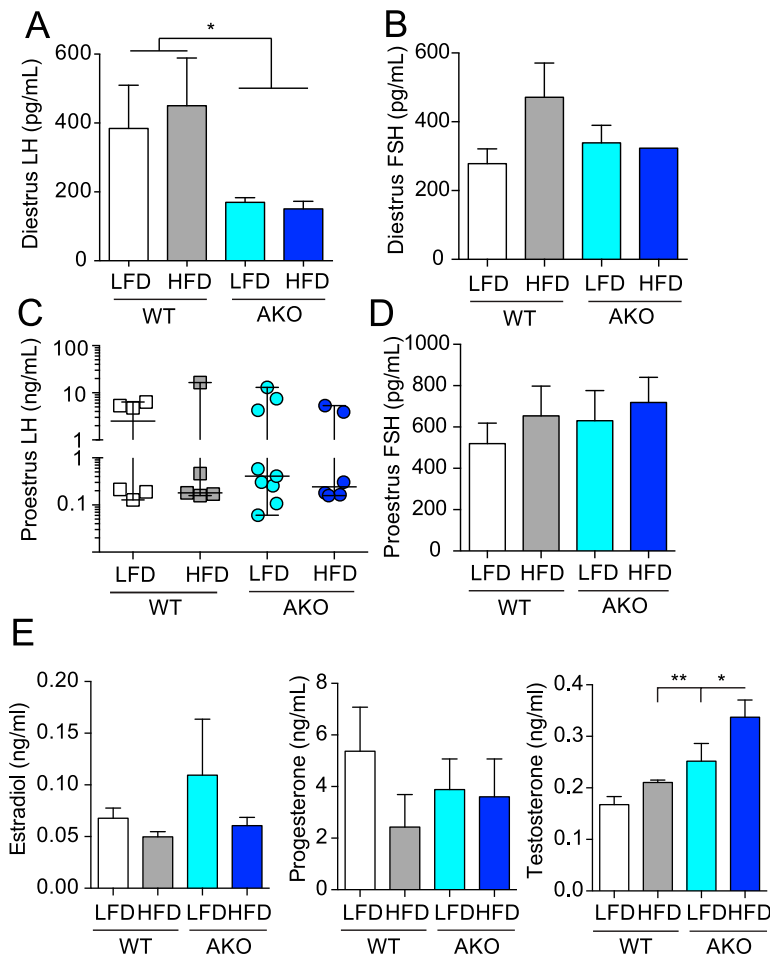

Figure 6. Effect of DIO and astrocyte PPARγ knockout on levels of plasma gonadotropins and steroids. (A) Plasma diestrus LH values for WT mice (n = 6, LFD group; n = 5, HFD group) and AKO mice (n = 9, LFD group; n = 6, HFD group). (B) Plasma diestrus FSH values. (C) Plasma proestrus LH values from samples taken at 6:00 PM on the day of proestrus. Individual, median, and range values are plotted. (D) Proestrus FSH values. (E) Diestrus estradiol, progesterone, and testosterone values. Testosterone shows a significant diet ($P < 0.05$) and genotype effect ($P < 0.01$) by two-way analysis of variance. Data are shown as mean $\pm$ standard error of the mean (n = 4, WT mice fed LFD; n = 4, WT mice fed HFD; n = 4, AKO mice fed LFD; n = 6, AKO mice fed HFD). *$P < 0.05$; **$P < 0.01$ for indicated *post hoc* comparisons.

G. Astrocyte-Specific Deletion of PPARγ Altered Hypothalamic and Ovarian Gene Expression and Gonadotropin Response to Kisspeptin Stimulation

The expression of various hypothalamic peptides involved in the regulation of reproduction was tested. Expression of *Npvf*, which encodes for RFRP-3; *Hcrt*, which encodes for orexin; and *Kiss1*, which encodes for kisspeptin, was increased in the hypothalamus of lean AKO mice compared with lean control mice. Obesity normalized expression to the levels of control mice [Fig. 7(A)]. Expression of receptors for neurokinin B (*Tac3r*) and RFRP3 (*Npffr1*) was significantly elevated in WT mice fed the HFD but not in AKO mice. In contrast, the kisspeptin receptor (*Gpr54*) and the cocaine and amphetamine-regulated transcript (*Cart*) showed genotype effects and expression was elevated in the AKO mice [Fig. 7(A)]. Expression of other neuropeptides, including *Gnrh, Tac2, Pdyn, Agrp, Pomc,* and *Avp*, did not significantly differ between groups (Supplemental Fig. 5A), nor did expression of the receptors for orexin (*Hcrtr1* and *Hcrtr2*), for the melanocortins (*Mc2r* and *Mc4r*), the k-opioid receptor for dynorphin (*Oprk1*), or the leptin receptor (*Lepr*; Supplemental Fig. 5B). No significant changes were seen in a panel of inflammatory genes (Supplemental Fig. 5C), indicating that loss of *Pparg* in astrocytes does not cause hypothalamic inflammation.

Gpr54 expression was altered in the AKO mice; therefore, a kisspeptin stimulation test was performed to test the response of the GnRH neurons. An acute bolus of kisspeptin-10 increased plasma LH levels in all groups [Fig. 7(B)], but the response was muted in the AKO mice fed the HFD. Plasma FSH levels also increased in response to kisspeptin in control mice, in contrast to the GnRH stimulation test [Fig. 4(D)], but the AKO mice did not show a FSH response to kisspeptin, although the HFD increased plasma FSH levels in this group [Fig. 7(C)].

Testosterone levels were altered in the AKO mice; therefore, we measured expression of steroidogenic genes in the ovary. Expression of the genes for aromatase (*Cyp19a1*), the FSH receptor (*Fshr*), and the steroidogenic acute regulatory protein (*Star*) were decreased in lean AKO mice, and obesity did not significantly modify this effect [Fig. 7(D)]. Other steroidogenic genes were not significantly altered in these groups (Supplemental Fig. 6).

3. Discussion

We report that loss of PPARγ expression in astrocytes in mice caused a metabolic derangement with mild hepatic steatosis and impaired glucose and insulin tolerance. Surprisingly, the metabolic phenotype did not worsen with DIO due to high-fat feeding; thus, obese AKO mice were significantly less glucose and insulin intolerant than obese WT littermates. Loss of PPARγ did not alter weight gain in mice fed either a LFD or HFD, although food consumption was lower in the AKO mice fed the LFD and these animals were not responsive to leptin-induced repression of food intake. The impaired glucose tolerance in the AKO mice was associated with increased expression of the gluconeogenic genes *Pcx, G6pc*, and *Pdk4*, and the hepatic steatosis was associated with increased expression of lipid synthesis, and uptake and storage genes (*i.e.*, *Acaca, Ldlr*, and *Cidec*). Expression of *Lipe* was also increased, suggesting that the triglyceride content in the lipid droplets is dynamic and that energy was derived from fatty acid oxidation. Peroxisomal and mitochondrial fatty acid oxidation expression of *Acox1, Ehhadh, Acaa1a, Acadvl*, and *Acadl* was decreased, however, to levels seen in obese mice, suggesting impaired function in the face of increased lipid oxidation.

How can these metabolic and gene expression changes be explained? We could not detect recombination of the *Pparg* allele in the liver, although *Gfap* is expressed in some stellate cells, so we believe the effect of the deletion is central. We saw no evidence of gliosis or elevated cytokine levels, so the changes do not appear to be related to hypothalamic inflammation. One possible explanation is that these metabolic and gene expression changes are caused by increased sympathetic output to the liver [38] because POMC and AgRP neurons control adipocyte lipolysis and liver metabolism via the melanocortin system and the sympathetic
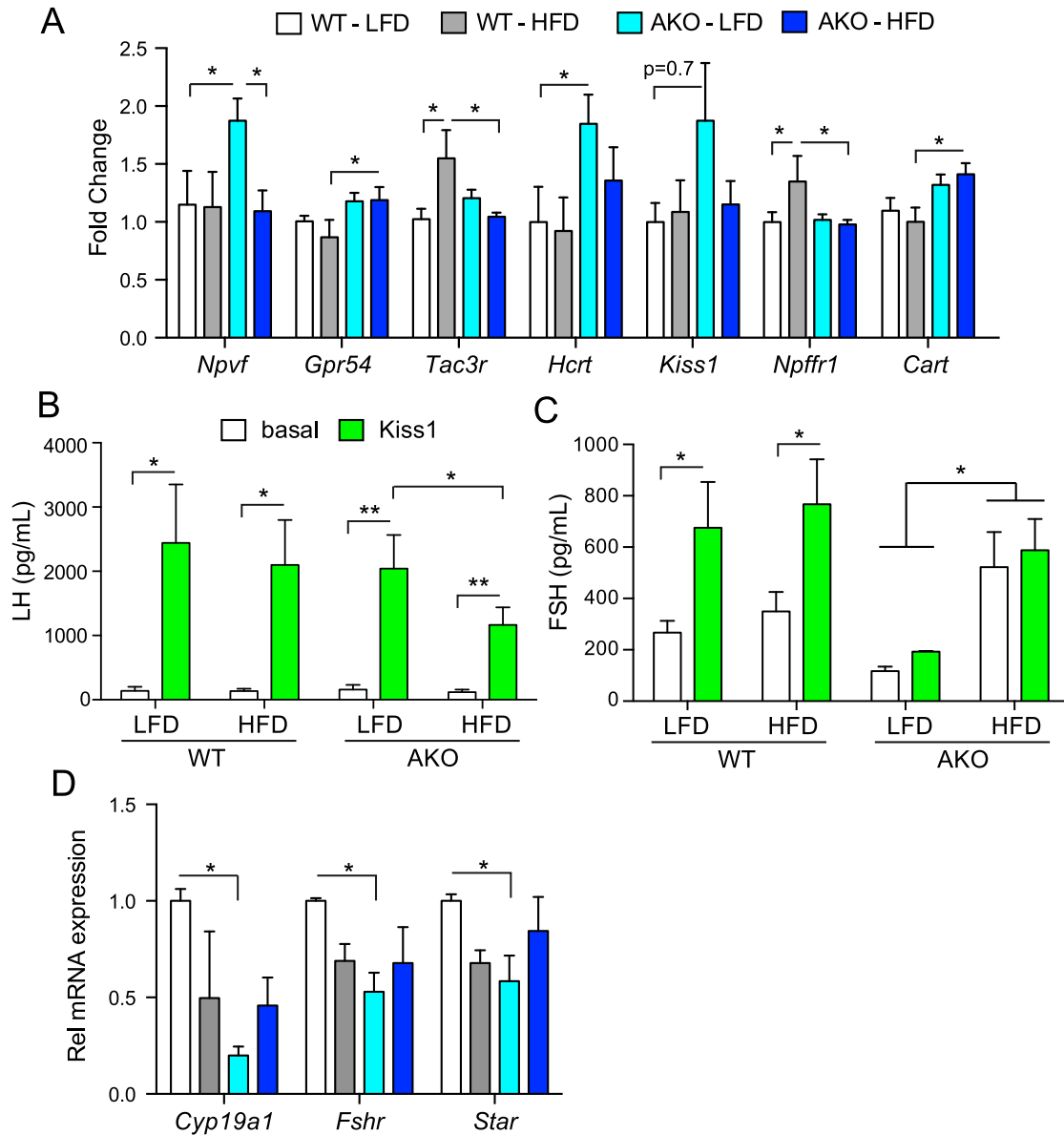
Figure 7. Effect of DIO and astrocyte PPARγ knockout on hypothalamic gene expression, kisspeptin response, and ovarian gene expression. (A) Gene expression was measured in RNA extracted from mouse hypothalamus quantitative PCR (qPCR; n = 7 WT-LFD; n = 6 WT-HFD; n = 6 AKO-LFD; n = 5 AKO-HFD). Expression of hypothalamic neuropeptides RFRP3 (*Npvf*), orexin (*Hcrt*), kisspeptin (*Kiss1*), of cocaine- and amphetamine-regulated transcript (*Cart*), and of the receptors for *Gpr5*), *Tac3r* and *Npffr1* was measured by qPCR. Data are presented as mean ± standard error of the mean. (B) Kisspeptin hypothalamic stimulation test. Mice received kisspeptin 10 (30 nmol) in the morning. Tail-vein blood samples were taken before (white bars) and 20 minutes after kisspeptin injection (green bars). Data are shown as mean ± standard error of the mean (n = 3 WT-LFD; n = 4 WT-HFD; n = 2 AKO-LFD; n = 4 AKO-HFD). Kisspeptin significantly stimulated plasma LH levels in WT and AKO mice, *P < 0.05; **P < 0.01. The HFD significantly attenuated the response in the AKO mice (*P < 0.05). Kisspeptin significantly stimulated FSH levels in WT mice (P < 0.05) but not in AKO mice. DIO significantly elevated FSH levels in AKO mice (P < 0.05). (C) Ovarian steroidogenic genes. Expression of *Cyp19a1*, *Fshr*, and *Star* were measured by qPCR (n = 4/group). *P < 0.05 for the indicated comparison. AKO-HFD, knockout mice fed the high-fat diet; AKO-LFD, knockout mice fed the low-fat diet; Rel, relative; WT-HFD, wild-type mice fed the high-fat diet; WT-LFD, wild-type mice fed the low-fat diet.

nervous system [39, 40]. A role for astrocytes in sympathetic output is supported by the observation that angiotensin II decreases glutamate transporter activity in astrocytes, leading to activation of NMDA receptors and enhanced sympathetic outflow [41]. Moreover, astrocyte activation inhibits AgRP neurons and feeding, via modulating extracellular levels of adenosine [42]. Insulin is a satiety factor and represses AgRP neurons; mice lacking the insulin receptor in AgRP neurons exhibit hepatic insulin resistance [43], and the fasting activation of AgRP neurons requires NMDA receptors and glutamatergic input [44].

What is PPARγ's role in astrocytes? On the one hand, PPARγ activation increases glucose uptake into astrocytes and increases lactate release to provide metabolic support for neurons [16, 45]. On the other hand, the glutamate transporter GLT-1 is a PPARγ target gene [36] and PPARγ activation reduces excitotoxicity by increasing glutamate uptake [46, 47], indicating a direct effect on neuronal activation. Loss of the glutamate transporter GLT-1 in astrocytes, but not neurons, causes a decrease in body weight, but the effect on food intake, energy expenditure, and liver metabolism was not studied [48]. Thus, it is intriguing to speculate that the reduced GLT-1 expression may increase glutamatergic signaling in AgRP neurons, causing hepatic insulin resistance via increased sympathetic output.

In addition to the metabolic phenotype, the female AKO mice had altered estrous cycles, with fewer corpora lutea and more early-stage follicles. LH surges appeared intact in the AKO mice, suggesting the reduced corpora lutea numbers were a result of impaired follicle development rather than an ovulation defect. Reproduction is regulated centrally through the hypothalamic kisspeptin-GnRH neural network. Although we did not find any differences in GnRH expression in the AKO mice, several other hypothalamic genes were altered. In particular, expression of *Npvf*, the homolog of avian gonadotropin-inhibiting hormone, and *Hcrt* were significantly elevated in the AKO mice. RFRP3 can directly inhibit gonadotropin production at the pituitary by interfering with GnRH signaling [29, 49] and, in some species, may inhibit the activity of GnRH neurons [27, 50, 51]. Similarly, orexins can inhibit pulsatile gonadotropin release at the pituitary or inhibit GnRH neuron activity [52–55]. It is not clear how loss of PPARγ in astrocytes would alter the expression of RFRP3 or HCRT, thus impairing the hypothalamic-pituitary-ovarian axis, but gliosis is associated with loss of HCRT neurons in people with narcolepsy [56]. Interestingly, RFRP3 immunoreactivity has been detected in astrocytes in the rat hippocampus, raising the possibility of direct astrocytic suppression of GnRH neuron activity [28]. We observed that the kisspeptin-GnRH neural network was partially disrupted in the AKO mice, because we did not observe an increase in plasma FSH levels after kisspeptin administration despite a normal LH response. A single administration of GnRH did not cause an increase in FSH level, as we and others have reported [37, 57], but kisspeptin administration caused a robust increase in FSH level [58]. Kisspeptin has no direct effect on FSH secretion from anterior pituitary cells [59], so the effect is likely central. Loss of GPR54 severely inhibits circulating LH and FSH levels [60], but, interestingly, residual kisspeptin effects on FSH levels were observed in GPR54$^{-/-}$ mice, suggesting other possible signaling pathways [61].

At the ovary level, we observed decreased *Cyp19a1*, *Fshr*, and *Star* expression but normal *Cyp17a1*, *Cyp11a1*, and *Lhr*. *Cyp17a1* and *Cyp11a1* are primarily expressed in theca cells and regulate testosterone production in response to LH [62]. In contrast, *Cyp19a1* and *Fshr* are expressed in granulosa cells and regulate conversion of testosterone to estradiol in response to FSH. The reduced expression of *Cyp19a1* was consistent with the decrease in *Fshr* expression, the increased numbers of early-stage follicles in the AKO mice, and the increased testosterone levels. It is not clear whether the alterations at the ovary are a result of changes to the hypothalamus-pituitary axis or due to direct innervation of the ovary [63], because sympathetic stimulation of the ovary decreases *Fshr* expression and inhibits ovarian estradiol production [64, 65]. Women with polycystic ovary syndrome also have autonomic dysfunction [66] with increased sympathetic tone [67, 68] and elevated testosterone to estradiol ratios [69]. So, the observations in the AKO mice could also be consistent with increased sympathetic output in addition to hypothalamic changes.

In conclusion, we have shown that PPARγ plays an important role in astrocytes and neurons in the CNS to regulate metabolic and reproductive pathways. In neurons, PPARγ's principal role was to modulate leptin sensitivity; however, in astrocytes, PPARγ maintains normal hepatic insulin sensitivity, prevents steatosis, and is important for the correct kisspeptin regulation of the hypothalamic-pituitary axis and estrous cycles. Additional detailed studies will be needed to dissect these metabolic and reproductive responses to identify the molecular and neuroendocrine pathways involved.

Acknowledgments

References and Notes

1. Ching J, Amiridis S, Stylli SS, Morokoff AP, O'Brien TJ, Kaye AH. A novel treatment strategy for glioblastoma multiforme and glioma associated seizures: increasing glutamate uptake with PPARγ agonists. *J Clin Neurosci.* 2015;**22**(1):21–28.

2. Quintanilla RA, Utreras E, Cabezas-Opazo FA. Role of PPAR γ in the differentiation and function of neurons. *PPAR Res.* 2014;**2014**:768594.

3. Fernandez MO, Sharma S, Kim S, Rickert E, Hsueh K, Hwang V, Olefsky JM, Webster NJ. Obese neuronal PPARγ knockout mice are leptin sensitive but show impaired glucose tolerance and fertility. *Endocrinology.* 2017;**158**(1):121–133.

4. Lu M, Sarruf DA, Talukdar S, Sharma S, Li P, Bandyopadhyay G, Nalbandian S, Fan W, Gayen JR, Mahata SK, Webster NJ, Schwartz MW, Olefsky JM. Brain PPAR-γ promotes obesity and is required for the insulin-sensitizing effect of thiazolidinediones. *Nat Med.* 2011;**17**(5):618–622.

5. Mandrekar-Colucci S, Sauerbeck A, Popovich PG, McTigue DM. PPAR agonists as therapeutics for CNS trauma and neurological diseases. *ASN Neuro.* 2013;**5**(5):e00129.

6. Di Giacomo E, Benedetti E, Cristiano L, Antonosante A, d'Angelo M, Fidoamore A, Barone D, Moreno S, Ippoliti R, Cerù MP, Giordano A, Cimini A. Roles of PPAR transcription factors in the energetic metabolic switch occurring during adult neurogenesis. *Cell Cycle.* 2017;**16**(1):59–72.

7. Warden A, Truitt J, Merriman M, Ponomareva O, Jameson K, Ferguson LB, Mayfield RD, Harris RA. Localization of PPAR isotypes in the adult mouse and human brain. *Sci Rep.* 2016;**6**:27618.

8. Hill JW, Elmquist JK, Elias CF. Hypothalamic pathways linking energy balance and reproduction. *Am J Physiol Endocrinol Metab.* 2008;**294**(5):E827–E832.

9. Roh E, Kim MS. Brain regulation of energy metabolism. *Endocrinol Metab (Seoul).* 2016;**31**(4):519–524.

10. Douglass JD, Dorfman MD, Thaler JP. Glia: silent partners in energy homeostasis and obesity pathogenesis. *Diabetologia.* 2017;**60**(2):226–236.

11. Azevedo FA, Carvalho LR, Grinberg LT, Farfel JM, Ferretti RE, Leite RE, Jacob Filho W, Lent R, Herculano-Houzel S. Equal numbers of neuronal and nonneuronal cells make the human brain an isometrically scaled-up primate brain. *J Comp Neurol.* 2009;**513**(5):532–541.

12. Jäkel S, Dimou L. Glial cells and their function in the adult brain: a journey through the history of their ablation. *Front Cell Neurosci.* 2017;**11**:24.

13. Barreto GE, Gonzalez J, Torres Y, Morales L. Astrocytic-neuronal crosstalk: implications for neuroprotection from brain injury. *Neurosci Res.* 2011;**71**(2):107–113.

14. Magistretti PJ. Neuron-glia metabolic coupling and plasticity. *Exp Physiol.* 2011;**96**(4):407–410.

15. Newman EA. New roles for astrocytes: regulation of synaptic transmission. *Trends Neurosci.* 2003;**26**(10):536–542.

16. Iglesias J, Morales L, Barreto GE. Metabolic and inflammatory adaptation of reactive astrocytes: role of PPARs. *Mol Neurobiol.* 2017;**54**(4):2518–2538.

17. Chowen JA, Argente-Arizón P, Freire-Regatillo A, Frago LM, Horvath TL, Argente J. The role of astrocytes in the hypothalamic response and adaptation to metabolic signals. *Prog Neurobiol*. 2016;**144**:68–87.

18. García-Cáceres C, Quarta C, Varela L, Gao Y, Gruber T, Legutko B, Jastroch M, Johansson P, Ninkovic J, Yi CX, Le Thuc O, Szigeti-Buck K, Cai W, Meyer CW, Pfluger PT, Fernandez AM, Luquet S, Woods SC, Torres-Alemán I, Kahn CR, Götz M, Horvath TL, Tschöp MH. Astrocytic insulin signaling couples brain glucose uptake with nutrient availability. *Cell*. 2016;**166**(4):867–880.

19. Kim JG, Suyama S, Koch M, Jin S, Argente-Arizon P, Argente J, Liu ZW, Zimmer MR, Jeong JK, Szigeti-Buck K, Gao Y, Garcia-Caceres C, Yi CX, Salmaso N, Vaccarino FM, Chowen J, Diano S, Dietrich MO, Tschöp MH, Horvath TL. Leptin signaling in astrocytes regulates hypothalamic neuronal circuits and feeding. *Nat Neurosci*. 2014;**17**(7):908–910.

20. Wang Y, Hsuchou H, He Y, Kastin AJ, Pan W. Role of astrocytes in leptin signaling. *J Mol Neurosci*. 2015;**56**(4):829–839.

21. Douglass JD, Dorfman MD, Fasnacht R, Shaffer LD, Thaler JP. Astrocyte IKKβ/NF-κB signaling is required for diet-induced obesity and hypothalamic inflammation. *Mol Metab*. 2017;**6**(4):366–373.

22. Buckman LB, Thompson MM, Lippert RN, Blackwell TS, Yull FE, Ellacott KL. Evidence for a novel functional role of astrocytes in the acute homeostatic response to high-fat diet intake in mice. *Mol Metab*. 2014;**4**(1):58–63.

23. Prevot V, Bellefontaine N, Baroncini M, Sharif A, Hanchate NK, Parkash J, Campagne C, de Seranno S. Gonadotrophin-releasing hormone nerve terminals, tanycytes and neurohaemal junction remodelling in the adult median eminence: functional consequences for reproduction and dynamic role of vascular endothelial cells. *J Neuroendocrinol*. 2010;**22**(7):639–649.

24. Prevot V, Hanchate NK, Bellefontaine N, Sharif A, Parkash J, Estrella C, Allet C, de Seranno S, Campagne C, de Tassigny Xd, Baroncini M. Function-related structural plasticity of the GnRH system: a role for neuronal-glial-endothelial interactions. *Front Neuroendocrinol*. 2010;**31**(3):241–258.

25. Rodríguez EM, Blázquez JL, Pastor FE, Peláez B, Peña P, Peruzzo B, Amat P. Hypothalamic tanycytes: a key component of brain-endocrine interaction. *Int Rev Cytol*. 2005;**247**:89–164.

26. Glanowska KM, Moenter SM. Endocannabinoids and prostaglandins both contribute to GnRH neuron-GABAergic afferent local feedback circuits. *J Neurophysiol*. 2011;**106**(6):3073–3081.

27. Ducret E, Anderson GM, Herbison AE. RFamide-related peptide-3, a mammalian gonadotropin-inhibitory hormone ortholog, regulates gonadotropin-releasing hormone neuron firing in the mouse. *Endocrinology*. 2009;**150**(6):2799–2804.

28. Ferris JK, Tse MT, Hamson DK, Taves MD, Ma C, McGuire N, Arckens L, Bentley GE, Galea LA, Floresco SB, Soma KK. Neuronal gonadotrophin-releasing hormone (GnRH) and astrocytic gonadotrophin inhibitory hormone (GnIH) immunoreactivity in the adult rat hippocampus. *J Neuroendocrinol*. 2015;**27**(10):772–786.

29. Shimizu M, Bédécarrats GY. Activation of the chicken gonadotropin-inhibitory hormone receptor reduces gonadotropin releasing hormone receptor signaling. *Gen Comp Endocrinol*. 2010;**167**(2): 331–337.

30. Tsutsui K, Bentley GE, Bedecarrats G, Osugi T, Ubuka T, Kriegsfeld LJ. Gonadotropin-inhibitory hormone (GnIH) and its control of central and peripheral reproductive function. *Front Neuroendocrinol*. 2010;**31**(3):284–295.

31. Clasadonte J, Poulain P, Hanchate NK, Corfas G, Ojeda SR, Prevot V. Prostaglandin E2 release from astrocytes triggers gonadotropin-releasing hormone (GnRH) neuron firing via EP2 receptor activation. *Proc Natl Acad Sci USA*. 2011;**108**(38):16104–16109.

32. Sandau US, Mungenast AE, McCarthy J, Biederer T, Corfas G, Ojeda SR. The synaptic cell adhesion molecule, SynCAM1, mediates astrocyte-to-astrocyte and astrocyte-to-GnRH neuron adhesiveness in the mouse hypothalamus. *Endocrinology*. 2011;**152**(6):2353–2363.

33. Hirrlinger PG, Scheller A, Braun C, Hirrlinger J, Kirchhoff F. Temporal control of gene recombination in astrocytes by transgenic expression of the tamoxifen-inducible DNA recombinase variant CreERT2. *Glia*. 2006;**54**(1):11–20.

34. He W, Barak Y, Hevener A, Olson P, Liao D, Le J, Nelson M, Ong E, Olefsky JM, Evans RM. Adipose-specific peroxisome proliferator-activated receptor gamma knockout causes insulin resistance in fat and liver but not in muscle. *Proc Natl Acad Sci USA*. 2003;**100**(26):15712–15717.

35. Hevener AL, He W, Barak Y, Le J, Bandyopadhyay G, Olson P, Wilkes J, Evans RM, Olefsky J. Muscle-specific Pparg deletion causes insulin resistance. *Nat Med*. 2003;**9**(12):1491–1497.

36. Romera C, Hurtado O, Mallolas J, Pereira MP, Morales JR, Romera A, Serena J, Vivancos J, Nombela F, Lorenzo P, Lizasoain I, Moro MA. Ischemic preconditioning reveals that GLT1/EAAT2 glutamate transporter is a novel PPARgamma target gene involved in neuroprotection. *J Cereb Blood Flow Metab*. 2007;**27**(7):1327–1338.

37. Sharma S, Morinaga H, Hwang V, Fan W, Fernandez MO, Varki N, Olefsky JM, Webster NJ. Free fatty acids induce Lhb mRNA but suppress Fshb mRNA in pituitary LβT2 gonadotropes and diet-induced obesity reduces FSH levels in male mice and disrupts the proestrous LH/FSH surge in female mice. *Endocrinology*. 2013;**154**(6):2188–2199.

38. Jensen KJ, Alpini G, Glaser S. Hepatic nervous system and neurobiology of the liver. *Compr Physiol*. 2013;**3**(2):655–665.

39. Brito MN, Brito NA, Baro DJ, Song CK, Bartness TJ. Differential activation of the sympathetic innervation of adipose tissues by melanocortin receptor stimulation. *Endocrinology*. 2007;**148**(11):5339–5347.

40. Geerling JJ, Boon MR, Kooijman S, Parlevliet ET, Havekes LM, Romijn JA, Meurs IM, Rensen PC. Sympathetic nervous system control of triglyceride metabolism: novel concepts derived from recent studies. *J Lipid Res*. 2014;**55**(2):180–189.

41. Stern JE, Son S, Biancardi VC, Zheng H, Sharma N, Patel KP. Astrocytes contribute to angiotensin II stimulation of hypothalamic neuronal activity and sympathetic outflow. *Hypertension*. 2016;**68**(6): 1483–1493.

42. Yang L, Qi Y, Yang Y. Astrocytes control food intake by inhibiting AGRP neuron activity via adenosine A1 receptors. *Cell Reports*. 2015;**11**(5):798–807.

43. Shin AC, Filatova N, Lindtner C, Chi T, Degann S, Oberlin D, Buettner C. Insulin receptor signaling in POMC, but not AgRP, neurons controls adipose tissue insulin action. *Diabetes*. 2017;**66**(6):1560–1571.

44. Liu T, Kong D, Shah BP, Ye C, Koda S, Saunders A, Ding JB, Yang Z, Sabatini BL, Lowell BB. Fasting activation of AgRP neurons requires NMDA receptors and involves spinogenesis and increased excitatory tone. *Neuron*. 2012;**73**(3):511–522.

45. Dello Russo C, Gavrilyuk V, Weinberg G, Almeida A, Bolanos JP, Palmer J, Pelligrino D, Galea E, Feinstein DL. Peroxisome proliferator-activated receptor gamma thiazolidinedione agonists increase glucose metabolism in astrocytes. *J Biol Chem*. 2003;**278**(8):5828–5836.

46. Verma R, Mishra V, Gupta K, Sasmal D, Raghubir R. Neuroprotection by rosiglitazone in transient focal cerebral ischemia might not be mediated by glutamate transporter-1. *J Neurosci Res*. 2011;**89**(11): 1849–1858.

47. García-Bueno B, Caso JR, Pérez-Nievas BG, Lorenzo P, Leza JC. Effects of peroxisome proliferator-activated receptor gamma agonists on brain glucose and glutamate transporters after stress in rats. *Neuropsychopharmacology*. 2007;**32**(6):1251–1260.

48. Petr GT, Sun Y, Frederick NM, Zhou Y, Dhamne SC, Hameed MQ, Miranda C, Bedoya EA, Fischer KD, Armsen W, Wang J, Danbolt NC, Rotenberg A, Aoki CJ, Rosenberg PA. Conditional deletion of the glutamate transporter GLT-1 reveals that astrocytic GLT-1 protects against fatal epilepsy while neuronal GLT-1 contributes significantly to glutamate uptake into synaptosomes. *J Neurosci*. 2015; **35**(13):5187–5201.

49. Sari IP, Rao A, Smith JT, Tilbrook AJ, Clarke IJ. Effect of RF-amide-related peptide-3 on luteinizing hormone and follicle-stimulating hormone synthesis and secretion in ovine pituitary gonadotropes. *Endocrinology*. 2009;**150**(12):5549–5556.

50. Ubuka T, Kim S, Huang YC, Reid J, Jiang J, Osugi T, Chowdhury VS, Tsutsui K, Bentley GE. Gonadotropin-inhibitory hormone neurons interact directly with gonadotropin-releasing hormone-I and -II neurons in European starling brain. *Endocrinology*. 2008;**149**(1):268–278.

51. Kriegsfeld LJ, Mei DF, Bentley GE, Ubuka T, Mason AO, Inoue K, Ukena K, Tsutsui K, Silver R. Identification and characterization of a gonadotropin-inhibitory system in the brains of mammals. *Proc Natl Acad Sci USA*. 2006;**103**(7):2410–2415.

52. Martynska L, Wolinska-Witort E, Chmielowska M, Kalisz M, Baranowska B, Bik W. Effect of orexin A on the release of GnRH-stimulated gonadotrophins from cultured pituitary cells of immature and mature female rats. *Neuropeptides*. 2014;**48**(4):199–205.

53. Furuta M, Mitsushima D, Shinohara K, Kimura F, Funabashi T. Food availability affects orexin a/ hypocretin-1-induced inhibition of pulsatile luteinizing hormone secretion in female rats. *Neuroendocrinology*. 2010;**91**(1):41–47.

54. Gaskins GT, Moenter SM. Orexin a suppresses gonadotropin-releasing hormone (GnRH) neuron activity in the mouse. *Endocrinology*. 2012;**153**(8):3850–3860.

55. Small CJ, Goubillon ML, Murray JF, Siddiqui A, Grimshaw SE, Young H, Sivanesan V, Kalamatianos T, Kennedy AR, Coen CW, Bloom SR, Wilson CA. Central orexin A has site-specific effects on luteinizing hormone release in female rats. *Endocrinology*. 2003;**144**(7):3225–3236.

56. Thannickal TC, Siegel JM, Nienhuis R, Moore RY. Pattern of hypocretin (orexin) soma and axon loss, and gliosis, in human narcolepsy. *Brain Pathol*. 2003;**13**(3):340–351.

57. Hashizume T, Saito H, Sawada T, Yaegashi T, Ezzat AA, Sawai K, Yamashita T. Characteristics of stimulation of gonadotropin secretion by kisspeptin-10 in female goats. *Anim Reprod Sci*. 2010;**118**(1):37–41.

58. Roa J, Vigo E, García-Galiano D, Castellano JM, Navarro VM, Pineda R, Diéguez C, Aguilar E, Pinilla L, Tena-Sempere M. Desensitization of gonadotropin responses to kisspeptin in the female rat: analyses of LH and FSH secretion at different developmental and metabolic states. *Am J Physiol Endocrinol Metab.* 2008;**294**(6):E1088–E1096.

59. Ezzat AA, Saito H, Sawada T, Yaegashi T, Goto Y, Nakajima Y, Jin J, Yamashita T, Sawai K, Hashizume T. The role of sexual steroid hormones in the direct stimulation by Kisspeptin-10 of the secretion of luteinizing hormone, follicle-stimulating hormone and prolactin from bovine anterior pituitary cells. *Anim Reprod Sci.* 2010;**121**(3-4):267–272.

60. Seminara SB, Messager S, Chatzidaki EE, Thresher RR, Acierno JS, Jr, Shagoury JK, Bo-Abbas Y, Kuohung W, Schwinof KM, Hendrick AG, Zahn D, Dixon J, Kaiser UB, Slaugenhaupt SA, Gusella JF, O'Rahilly S, Carlton MB, Crowley WF, Jr, Aparicio SA, Colledge WH. The GPR54 gene as a regulator of puberty. *N Engl J Med.* 2003;**349**(17):1614–1627.

61. García-Galiano D, van Ingen Schenau D, Leon S, Krajnc-Franken MA, Manfredi-Lozano M, Romero-Ruiz A, Navarro VM, Gaytan F, van Noort PI, Pinilla L, Blomenröhr M, Tena-Sempere M. Kisspeptin signaling is indispensable for neurokinin B, but not glutamate, stimulation of gonadotropin secretion in mice. *Endocrinology.* 2012;**153**(1):316–328.

62. Liu YX, Hsueh AJ. Synergism between granulosa and theca-interstitial cells in estrogen biosynthesis by gonadotropin-treated rat ovaries: studies on the two-cell, two-gonadotropin hypothesis using steroid antisera. *Biol Reprod.* 1986;**35**(1):27–36.

63. Domínguez R, Cruz-Morales SE. The ovarian innervation participates in the regulation of ovarian functions. *Endocrinol Metabol Syndrome.* 2011;**S4**:001.

64. Fernandois D, Cruz G, Na EK, Lara HE, Paredes AH. Kisspeptin level in the aging ovary is regulated by the sympathetic nervous system. *J Endocrinol.* 2017;**232**(1):97–105.

65. Uchida S, Kagitani F. Sympathetic regulation of ovarian functions under chronic estradiol treatment in rats. *Auton Neurosci.* 2016;**197**:19–24.

66. Abu Hashim H. Twenty years of ovulation induction with metformin for PCOS; what is the best available evidence? *Reprod Biomed Online.* 2016;**32**(1):44–53.

67. Ribeiro VB, Kogure GS, Reis RM, Gastaldi AC, DE Araújo JE, Mazon JH, Borghi A, Souza HC. Polycystic ovary syndrome presents higher sympathetic cardiac autonomic modulation that is not altered by strength training. *Int J Exerc Sci.* 2016;**9**(5):554–566.

68. Lansdown A, Rees DA. The sympathetic nervous system in polycystic ovary syndrome: a novel therapeutic target? *Clin Endocrinol (Oxf).* 2012;**77**(6):791–801.

69. Azziz R, Carmina E, Chen Z, Dunaif A, Laven JS, Legro RS, Lizneva D, Natterson-Horowtiz B, Teede HJ, Yildiz BO. Polycystic ovary syndrome. *Nat Rev Dis Primers.* 2016;**2**:16057.